Adsorption and Reaction of Ammonia on the Ru(11$\bar{2}$0) Surface†

Y. Wang and K. Jacobi*

Fritz-Haber-Institut der Max-Planck-Gesellschaft, Faradayweg 4-6, D-14195 Berlin, Germany

Received: February 4, 2004; In Final Form: June 23, 2004

The adsorption and reaction of NH_3 was studied on the Ru(11$\bar{2}$0) surface using high-resolution electron energy loss spectroscopy and thermal desorption spectroscopy. Following NH_3 exposure at 85 K, annealing to 140 K leads to desorption of the multilayer and second layer leaving the NH_3 monolayer which is characterized by two adsorption states: α_1-NH_3 at a 3-fold hollow site and a more weakly bonded α_2-NH_3 at an on-top site. As the temperature is increased, the α_2-NH_3 desorbs molecularly, while partial dehydrogenation occurs for the α_1-NH_3. This process proceeds at 3-fold hollow sites in successive steps finally leading to atomic nitrogen. The bonding competition effect accounts for the low N coverage of 0.11 ML obtained following NH_3 exposure at 85 K and annealing. The activation barrier for associative desorption of nitrogen is estimated to be 120 ± 20 kJ/mol. At 300 K, the anticipated NH_3 synthesis from successive hydrogenation of adsorbed N is observed.

1. Introduction

There is general consensus that the synthesis of ammonia over the industrial iron-based catalyst proceeds via stepwise recombination of chemisorbed nitrogen and hydrogen whereby the dissociative chemisorption of N_2 represents the rate-limiting step.[1] An analogous mechanism is also expected for Ru catalysts, which may become the second-generation industrial catalysts for NH_3 synthesis.[2,3] Since the details of the reactions involved are not established yet, we have set up some experiments on Ru single-crystal surfaces.

The first experiments on the adsorption of NH_3 on Ru(0001) have been carried out by Danielson and co-workers,[4,5] and they have shown that NH_3 desorbs reversibly for adsorption temperatures below 300 K. The desorption has been found to be complete at about 350 K. Two different desorption states have been distinguished in the monolayer regime by others.[6] Dissociation of NH_3 on Ru(0001) has been achieved by electron bombardment[5] or by exposing the surface to large fluences of NH_3 with the surface temperature maintained above 300 K.[7,8] The vibrational frequencies for the monolayer, second-layer, and multilayer NH_3 on Ru(0001) have been reviewed by Parmeter et al.[9] who suggested that NH_3 adsorbs in an on-top site. Decomposition of NH_3 upon heating has been observed on a stepped Ru(1 1 10) surface by Egawa et al.[8]

On our way to elucidate the mechanism and the kinetics of NH_3 synthesis on Ru single-crystal surfaces, the chemisorption and interaction of hydrogen and nitrogen on Ru(0001) were investigated first.[10,11] The initial sticking coefficient for dissociative adsorption of N_2 was found to be $(1 \pm 0.8) \times 10^{-12}$ independent of surface orientation within the limits of error.[12] This contra-intuitive observation has been explained in the meantime through the observation—confirmed in ab initio density functional theory (DFT) calculations—of the high efficiency of the (001)-like steps on Ru(0001) being especially effective in N_2 dissociation.[13] Our conclusions from UHV-based studies on Ru surfaces have been summarized elsewhere.[14]

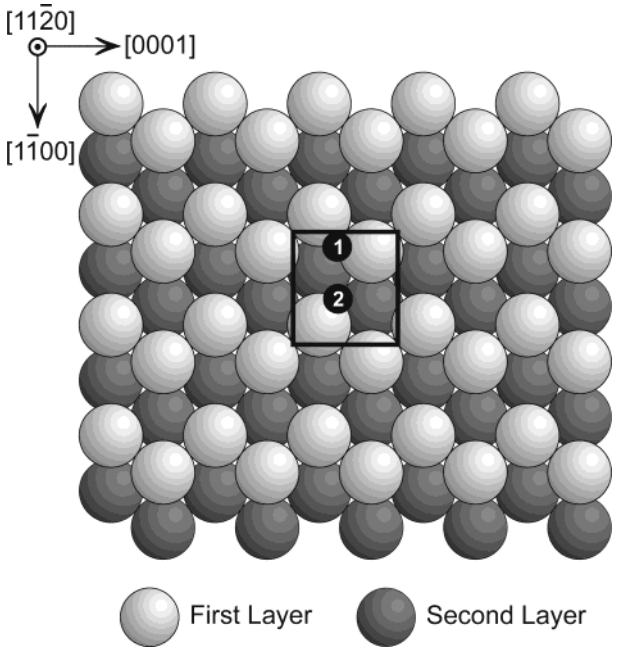

Figure 1. Top view of the Ru(11$\bar{2}$0) surface. Two atom layers are shown. The two different 3-fold hollow sites numbered 1 and 2 within the (1 × 1) unit cell are indicated.

In principle, the surface morphology of the small metal clusters, which act as catalysts, has to be taken into consideration. Generally, it is assumed that the more open surfaces are more reactive. In order to study a well-defined, open Ru surface, we have chosen here a Ru(11$\bar{2}$0) surface for which a schematic sketch of the ideal, bulk truncated 1 × 1 surface is shown in Figure 1. Although a surface structure determination does not exist yet, the 1 × 1 pattern observed in low-energy electron diffraction (LEED)[15] suggests that there is no reconstruction. Certainly, one expects some relaxation of the surface atoms which are known from other metal surfaces to be on the order of a few percent of the lattice constant. Therefore, the models of adsorption sites, which we propose in this contribution, rest upon the assumption of the bulk truncated 1 × 1 structure for the bare surface. Ru(11$\bar{2}$0) is less open than Ru(11$\bar{2}$1)[16] and

† Part of the special issue "Gerhard Ertl Festschrift".

* Corresponding author. Phone: +49-30-8413-5201. Fax: +49-30-8413-5106. E-mail: jacobi@fhi-berlin.mpg.de.

10.1021/jp049496n CCC: $27.50
Published on Web 08/27/2004

owns a mirror plane parallel to [1$\bar{1}$00] and a mirror glide plane parallel to [0001]. It is characterized by zigzag chains along the [0001] direction, separated by zigzag troughs, and two different 3-fold hollow sites (numbered 1 and 2) within the 1 × 1 unit cell. These sites are very likely to be active in the adsorption of atoms or molecules. The second-layer atoms lie deeper by 0.137 nm.

Recently, we have studied some details of the adsorption of ammonia on Ru(11$\bar{2}$0)[17,18] and have found that heating the sample to higher temperatures leads to thermal dehydrogenation in three successive steps as proven by three separate desorption peaks of hydrogen[17] and the observation of the NH_2 and NH reaction intermediates in HERRLS.[18] Besides these results, the following important problems have been left open for further discussion: (i) the characterization of the NH_3 monolayer, (ii) the identification of the site at which NH_3 dehydrogenation takes place, (iii) a deeper understanding of why, following annealing of the full NH_3 monolayer, only a low nitrogen coverage of 0.11 ML is achieved,[17] and (iv) NH_3 synthesis from N and H. Particularly, the identification of the adsorption site, which is still under discussion for single-crystal Ru surfaces, is very important for a deeper understanding of the decomposition process at an atomic level.

In this contribution we report on high-resolution electron energy loss spectroscopy (HREELS) and thermal desorption spectroscopy (TDS) of the interaction of NH_3 with Ru(11$\bar{2}$0). We demonstrate that there are two different adsorption sites of NH_3 in the monolayer. Dehydrogenation occurs only for NH_3 adsorbed at the 3-fold hollow sites. This process will be discussed in terms of the bonding competition effect. We also show that NH_3 can be synthesized again from stepwise hydrogenation of adsorbed N atoms at 300 K.

2. Experimental Section

The HREELS experiments were performed in an ultrahigh vacuum (UHV) apparatus consisting of two chambers separated by a valve. The base pressure was 2×10^{-11} mbar. The upper chamber was equipped with an argon ion gun, a quadrupole mass spectrometer for TDS, and a LEED optics; the lower chamber housed a HREEL spectrometer of the commercial Ibach design (Delta 0.5, SPECS, Germany). HREEL spectra were taken in specular geometry at an angle of incidence of 55° with respect to the surface normal. The primary electron beam energy was set to 3 eV, and the energy resolution was better than 2.5 meV.

The Ru(11$\bar{2}$0) sample, clamped between two W wires in narrow slits, was heated by electron bombardment from the backside and could be cooled to 85 K by liquid nitrogen; its temperature was measured with a Ni−CrNi thermocouple spot-welded to the edge of the sample. The substrate surface was prepared by cyclic argon ion bombardment with subsequent annealing to 1500 K. A sharp bright (1 × 1) pattern was observed in LEED for the clean surface.[15] HREELS was employed to check the cleanliness of the surface. $^{14}NH_3$ and $^{15}ND_3$ exposures are given in units of Langmuir (L) (1 L = 1.33×10^{-6} mbar·s). The gas purity was 99.98% for $^{14}NH_3$, 99.0% for ^{15}N, and 99.0% for D in $^{15}ND_3$. The coverage is given with respect to the number of substrate surface atoms.

3. Results

3.1. NH_3 Adsorption at 85 K. In Figure 2, TD spectra of NH_3 are shown for different exposures. After the first exposure of 0.08 L, no NH_3 desorption occurs. Increasing exposure leads to the appearance of a very small desorption peak at about 330 K which shifts to 300 K with further exposure. This can be explained by repulsive lateral interaction of the neighboring NH_3 molecules which results in a decrease of the desorption energy. At an exposure of 1 L the α_1-NH_3 state is completely filled, and the α_2-NH_3 state develops at about 200 K, accompanied by the appearance of the β state at 130 K. With an increase of the exposure to 5 L, the β state grows and shifts to 120 K, while the γ state is observed at 105 K. The TD spectra are quite similar to those forRu(11$\bar{2}$1)[16] and Ru(0001).[6] Therefore, we attribute the β and γ states to second-layer and multilayer ammonia, respectively.

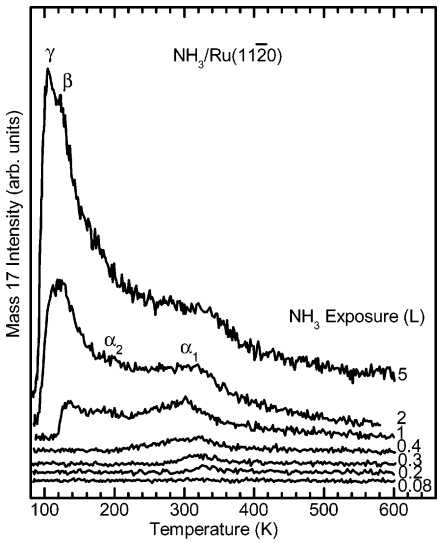

Figure 2. TD spectra of NH_3 (mass 17) for various NH_3 exposures to Ru(11$\bar{2}$0) at 85 K. The heating rate was 3 K/s.

The missing NH_3 TD peak for exposures smaller than 0.2 L suggests that NH_3 is completely dehydrogenated through interaction with the surface as proven by the observation of the desorption peaks of products hydrogen and nitrogen in TDS.[17] Before we present the results for the thermal evolution of chemisorbed ammonia, we will study the NH_3 monolayer in detail.

3.2. The NH_3 Monolayer. The NH_3 monolayer was prepared by exposing 2 L of NH_3 at 85 K and annealing to 140 K which releases the multilayer and second-layer NH_3 according to the TDS results (Figure 2). In order to unambiguously identify the NH_3-related vibrational modes, isotope substitution measurements with $^{15}ND_3$ were performed. Figure 3 exhibits the corresponding spectra for the $^{14}NH_3$ and $^{15}ND_3$ monolayers. In Table 1 the vibrational frequencies are summarized including the respective assignments and isotope shifts. From the isotope shifts one can clearly differentiate between translational and rotational modes.

Remarkable is the low-lying symmetric N−H stretching mode $\nu_s(NH_3)$ at 390 meV as compared to the same mode for Ru(0001) at 404 meV.[9] The charge transfer from the N lone pair ($^3a_1$ orbital) to Ru leads to a weakening of the intramolecular N−H bond as supported by observations for metal−NH_3 compounds.[19] The larger red-shift at Ru(11$\bar{2}$0) compared to the gas phase value (414 meV)[20] points to a stronger Ru−N bond. This effect works also for the $\delta_a(NH_3)$ mode observed at 191.5 meV exhibiting a red-shift of 5.5 meV with respect to the value for Ru(0001).[9]

The umbrella mode $\delta_S(NH_3)$ = 134 meV dominates the spectrum. (Note the change in the sensitivity factor.) The isotope shift of 1.29 is relatively small pointing to some coupling to translation modes. A coupling between modes is effective if

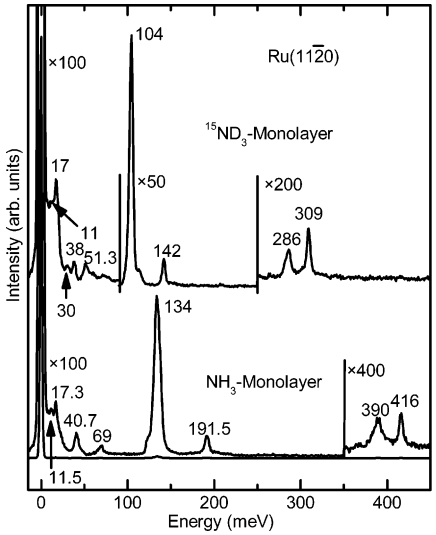

Figure 3. HREEL spectra of the NH_3 and the $^{15}ND_3$ monolayer on Ru(11$\bar{2}$0) prepared by exposing 2 L of NH_3 ($^{15}ND_3$) at 85 K and subsequently annealing to 140 K in order to desorb the multilayer and second layer. All spectra were recorded at 85 K in specular geometry with an incidence angle of 55° with respect to the surface normal and with a primary energy of 3 eV.

TABLE 1: Mode Assignments, Vibrational Frequencies in Units of meV, and Isotope Shifts for $^{14}NH_3$ and $^{15}ND_3$ on Ru(11$\bar{2}$0)[a]

mode	NH_3 [meV]	$^{15}ND_3$ [meV]	isotope shift
$T_{\parallel}(NH_3)$	11.5	11	1.05
$T_{\perp 1}(NH_3)$	17.3	17	1.02
$T_{\perp 2}(NH_3)$	40.7	38	1.07
$R_{xy1}(NH_3)$	40.7	30	1.35
$R_{xy2}(NH_3)$	69	51.3	1.35
$\delta_s(NH_3)$	134	104	1.29
$\delta_a(NH_3)$	191.5	142	1.35
$\nu_s(NH_3)$	390	286	1.36
$\nu_a(NH_3)$	416	309	1.35

[a] T, translational mode, || and ⊥ to the surface plane; R, libration mode; δ_s and δ_a, symmetric and asymmetric deformation modes; ν_s and ν_a, symmetric and asymmetric stretching modes.

components of the atomic movement point into the same direction. In case of the $\delta_S(NH_3)$ mode this would be the $T_{\perp}$-(NH_3) mode.

In the low-energy regime, the loss at 40.7 meV is assigned to a frustrated translation as concluded from the isotope shift of 1.07 for $^{15}ND_3$ (38.0 meV). We ascribe this mode to the $T_{\perp 2}(NH_3)$ mode normal to the surface since it lies at relatively high energy. There may also be a weak libration mode L_{xy1} at the same energy as derived from an additional mode at 30 meV for $^{15}ND_3$ and in agreement with the result for Ru(11$\bar{2}$1).[16]

Most importantly, for very low energies two losses at 11.5 and 17.3 meV are observed and explained as translation modes from the isotope shifts of 1.02−1.05. The observation of the isotope shifts clearly rules out an assignment to surface phonons. Actually, the latter are observed at 15, 25, and 30 meV with very weak intensity as shown below in Figure 6 (after annealing to 700 K). Both the observed isotope shift and the comparatively low intensity of the bare surface phonon modes indicate that the losses at 11.5 and17.3 meV are NH_3-derived and not Ru-derived (phonon) modes. The loss at 11.5 meV may be due to a frustrated translation $T_{\parallel}(NH_3)$ parallel to the surface similarly as found for Fe(110) by He atom scattering experiments.[21] Due to its high intensity, the 17.3 meV mode is assigned to a second $T_{\perp 1}(NH_3)$ mode. On Ru(11$\bar{2}$1) this mode is as intensive as the

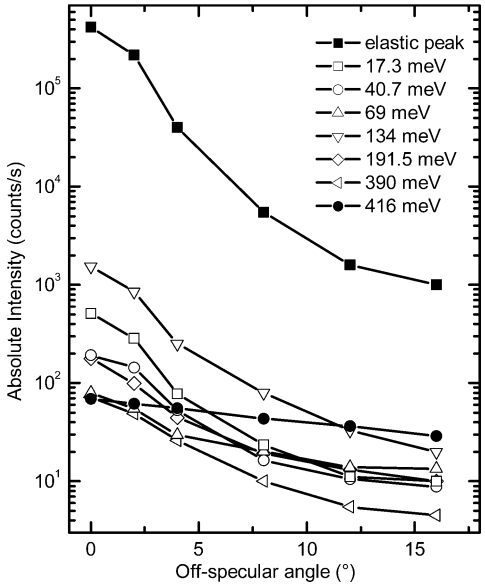

Figure 4. Absolute intensities of the elastically scattered electrons and the vibrational losses of the NH_3 monolayer on Ru(11$\bar{2}$0) as function of the off-specular angle.

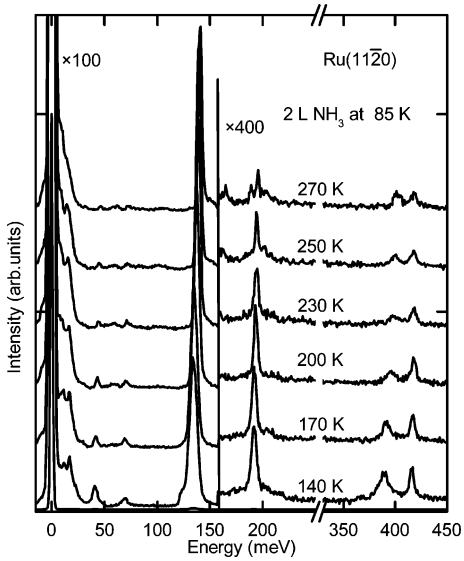

Figure 5. HREEL spectra for the NH_3 monolayer after exposing the Ru(11$\bar{2}$0) surface to 2 L of NH_3 and annealing to the indicated temperatures. Parameters as for Figure 3.

$\delta_S(NH_3)$ mode.[16] Also, on Ru(0001) such a low-lying mode was observed at 17.4 meV for the dilute NH_3 monolayer and was assigned to the 3-fold hollow site.[22] Interestingly, the authors briefly mentioned another T_Z mode at 44 meV for higher coverage which they ascribed to the on-top site without further discussion.[22] These results are in very good agreement with our finding and in line with the general belief that vibration frequencies depend on the local site symmetry rather than on surface symmetry. The low-lying mode at Ru(0001) is only of weak intensity. Obviously, the $T_{\perp}(NH_3)$ mode intensity depends strongly on the substrate surface, i.e., on the orientation of the site relative to the substrate.

To gain an insight into the adsorption geometry of NH_3, the dependence of the loss intensity on the off-specular angle is measured for the full monolayer as shown in Figure 4. All modes are dominated by dipole scattering. The only exception is the $\nu_a(NH_3)$ mode which is only weakly dipole active. Since all possible vibrational modes are observed, a C_{3v} symmetry, in

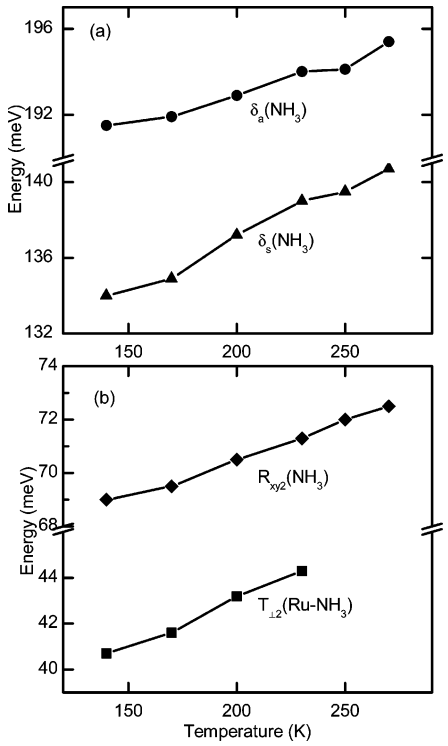

Figure 6. Energy of the vibrational modes of the NH_3 monolayer on Ru(11$\bar{2}$0) as a function of temperature. T, translational mode; R, rotational mode; δ, deformation mode.

which the 3-fold axis of the NH_3 species would be perpendicular to the surface, and some modes would be forbidden for symmetry reasons, can be excluded. Therefore, NH_3 must be tilted relative to the surface normal. This orientation can be accounted for by a repulsive lateral interaction between neighboring NH_3 molecules. Furthermore, from the geometrical structure of the Ru(11$\bar{2}$0) surface a tilt is also very likely, since the two 3-fold hollow sites, depicted in Figure 1, are both tilted with respect to the surface plane.

In summary, NH_3 adsorbs molecularly on Ru(11$\bar{2}$0) at 85 K. All expected vibrational modes for the NH_3 monolayer are identified. The finding of the two $T_\perp(NH_3)$ modes at 17.3 and 40.7 meV is important and will be discussed in detail in section 4.

3.3. Thermal Evolution of Chemisorbed NH_3. In order to further examine the interaction of ammonia with the Ru(11$\bar{2}$0) surface, the sample was exposed to 2 L of NH_3 at 85 K and subsequently annealed to different temperatures. The corresponding HREEL spectra are gathered in Figures 5 and 7. The measurements were performed always at 85 K in order to avoid the reactions from proceeding further. After annealing to 140 K, the spectrum exhibits the typical losses of chemisorbed NH_3. With stepwise heating to higher temperatures the $T_{\perp 2}(NH_3)$ mode at 40.7 meV decreases continually in intensity, whereas the intensity of the $T_{\perp 1}(NH_3)$ mode at 17.3 meV remains unchanged. Finally at 250 K, the $T_{\perp 2}(NH_3)$ peak disappears, corresponding to the desorption of the α_2 state in TDS (see Figure 2); the residual intensity at 43 meV is likely to be due to the hidden libration mode mentioned already. It should be noted that at this temperature all peaks are still related to NH_3 indicating that no reaction has taken place yet.

With heating to higher temperatures, i.e., with decreasing NH_3 coverage, most modes exhibit blue-shifts in energy as shown in Figure 6 and also summarized in Table 2. The $\delta_S(NH_3)$ mode shifts by 7 meV during warming to 250 K. From the comparison

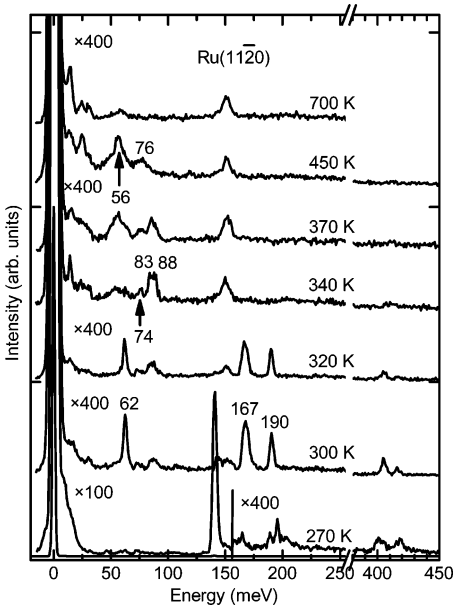

Figure 7. HREEL spectra for the NH_3 monolayer on the Ru(11$\bar{2}$0) surface. The curve at 270 K is identical to the respective curve in Figure 5. For the data set for annealing temperatures at and above 300 K 1 L of NH_3 was exposed at 85 K and annealed to the indicated temperatures. Actually, at 300 K only the α_1 state can be filled and saturation is already reached at 0.4 L. The curves at 300, 340, and 450 K have been presented already elsewhere.[17] Parameters as for Figure 3.

TABLE 2: Frequency Shifts of the Vibrational Modes for the NH_3 Monolayer after Annealing to 250 K[a]

modes	$T_{\perp 1}(NH_3)$	$T_{\perp 2}(NH_3)$	$R_{xy2}(NH_3)$	$\delta_s(NH_3)$	$\delta_a(NH_3)$	$\nu_s(NH_3)$
frequency shifts [meV]	−3	+4	+3.5	+7	+4	+11

[a] + indicates a blue-shift; − indicates a red-shift.

with metal−NH_3 compounds, Parmeter et al.[9] explained such a blue-shift considering the charge at the Ru surface atom to be changed: a more positive charge at Ru leads to a higher mode frequency. Besides for the $\delta_S(NH_3)$ mode one expects similar shifts for the $R(NH_3)$ and $T_\perp(NH_3)$ modes since they are also charge sensitive. Because of the low intensity, this could not be found for Ru(0001),[9] whereas the anticipated energy shifts were unambiguously observed here on Ru(11$\bar{2}$0) for the $T_{\perp 2}$-(NH_3) and $R_{xy}(NH_3)$ modes (see Figure 7 and Table 2). It is interesting to note a recent interpretation that at least part of the blue-shift of the δ_S mode on Ru(0001) may be due to a Stark effect produced by the static NH_3 dipoles within the adlayer.[22]

In contrast to $T_{\perp 2}$, the $T_{\perp 1}$ mode shifts down by 3 meV after annealing to 250 K. The origin of this red-shift can be explained as a dipole−dipole interaction between NH_3 molecules. Finally, we note that the $\nu_s(NH_3)$ mode shows a drastic blue-shift of 11 meV, which cannot be explained as due to a charge transfer or Stark effect. The origin of the blue-shift is not understood yet.

Upon further annealing to 270 K (see Figures 5 and 7), two weak losses at 167 and 190 meV are observed, accompanied by the decrease of the α_1-NH_3-related modes. The new peaks are characteristic for the NH_2 species,[18] indicating that NH_3 dehydrogenation is starting. After annealing to 300 K (Figure 7) the NH_3-related modes disappear completely revealing the desorption and/or dehydrogenation of NH_3. The spectrum now exhibits very well-resolved NH_2-related losses which are assigned to the frustrated translation mode (62 meV), the frustrated rotation (rocking) mode (167 meV), the bending or

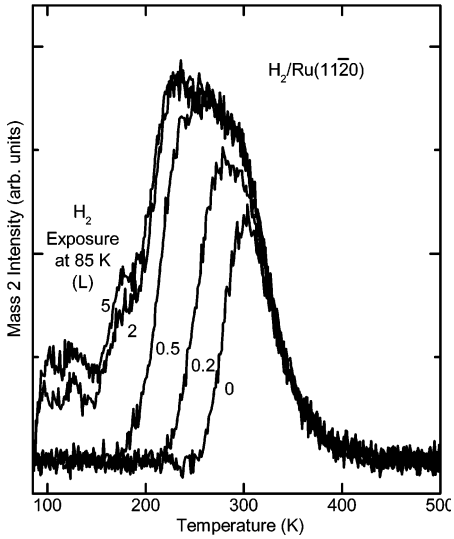

Figure 8. H_2 TD spectra (mass 2) for indicated H_2 exposures to Ru(11$\bar{2}$0) at 85 K.

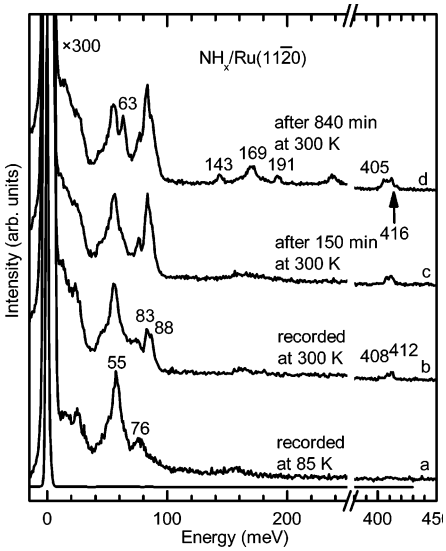

Figure 9. HREEL spectra of atomic N on Ru(11$\bar{2}$0) prepared by exposing 5 L of NH_3 at 300 K to the sample and annealing to 450 K. The spectra were taken (a) at 85 K and (b) at 300 K, (c) after 2.5 h in UHV at 300 K, and (d) after 14 h in UHV at 300 K. Parameters as for Figure 3.

scissoring mode (190 meV), and the symmetric (405 meV) and asymmetric (417 meV) stretching modes, respectively.[18]

By heating to 320 K, the NH_2-related losses decrease in intensity and vanish completely at 340 K. The spectrum is now characteristic for the NH species with the frustrated translation mode $T_\perp$(Ru−NH) at 74.1 meV as well as to the NH bending modes δ(NH) at 83 and 88 meV.[18] Note that the peak observed at about 150 meV is due to atomic hydrogen from dissociative adsorption of residual H_2 in the chamber during cooling of the sample down to 85 K since this mode increases in intensity with the time elapsed during the collection of the HREEL spectra. Hydrogen from the residual gas is also detected by TDS (see Figure 8 below).

Heating to 450 K leads to complete dehydrogenation as demonstrated by the disappearance of the NH-related modes. Some atomic N is left at the surface. Here we observe mainly two losses at 56 and 76 meV which are assigned to the ν(N−Ru) stretching modes at the two different 3-fold hollow sites of the 1×1 unit cell. A more intense spectrum measured after NH_3 reaction at 300 K will be presented below in Figure 9. By annealing to 700 K the N-related losses disappear completely corresponding to the associative desorption of adsorbed N atoms. The spectrum now exhibits the phonons at 15, 25, and 30 meV of the clean Ru(11$\bar{2}$0) surface.

3.4. NH_3 Synthesis. By taking into account the microscopic reversibility of elemental steps involved in the NH_3 dehydrogenation reaction, considerable insight into the ammonia synthesis can be obtained. Before we present the results for NH_3 synthesis, we have to ask whether hydrogen is available at the surface at 300 K. The respective TD spectra for different exposures at 85 K are shown in Figure 8. The general features observed in the case of H_2 adsorption are characterized by second-order desorption peaks shifting from 300 to 230 K. The first spectrum is from H_2 adsorption out of the residual gas which cannot be avoided even for a total pressure as low as 2×10^{-11} mbar. Figure 8 demonstrates that at 300 K hydrogen is available in amounts appropriate to enable reactions with other surface species.

Actually, we observed here NH_3 synthesis from stepwise hydrogenation of adsorbed N and H atoms as shown in Figure 9. First, a N-covered surface was prepared by exposing the Ru(11$\bar{2}$0) surface to 5 L of NH_3 at 300 K followed by warming to 450 K. The respective HREEL spectrum is shown in Figure 9, curve a. The two Ru−N stretching modes at 55 and 76 meV are found here with higher intensities than those in Figure 7. Even warming to 300 K leads to the formation of the first amounts of NH—as demonstrated by the two δ(NH) modes at 83 and 88 meV—just by reaction of N and H the latter from H_2 in the residual gas (see the discussion of Figure 8 above). With time the NH intensity grows, whereas the N-related losses decrease in intensity. The observation of two N−H stretching modes at 408 and 412 meV further reveals the occupation of two different adsorption sites for NH.

Exposure overnight to the residual gas (Figure 9, curve d) leads finally to the clear indication of NH_2 with peaks at 63, 169, 191, 405, and 416 meV. Even a measurable amount of NH_3 at 143 meV is measured. Much more NH_3 is not expected under these conditions, as we have shown above that NH_3 is not stable at room temperature; instead, not all N atoms become reacted off since the expected and essential neighboring adsorption sites are blocked by NH_2.

Finally we note that a reaction from the residual gas is certainly somewhat problematic especially with respect to some readsorption of NH_3. However, we believe that our data are reliable for the following reasons: (i) At 300 K (the temperature overnight) NH_3 decomposes only to NH_2 as known from our former work.[17] On the other hand, in our experiment presented here we observe the formation of NH first. (ii) The amount of atomic N at the surface decreases during the reaction with H overnight. This should not be the case if the NH_x species would result from readsorption of NH_3 from the residual gas. Therefore, we conclude that readsorption of NH_3 does not play a role.

4. Discussion

The HREELS result of two $T_\perp(NH_3)$ modes at 17.3 and 40.7 meV reveals that NH_3 is adsorbed at two different sites in the monolayer on Ru(11$\bar{2}$0). There is a quite general trend: the larger the coordination the smaller the vibrational energy.[20] Thus, we suggest that, in case of Ru(11$\bar{2}$0), ammonia adsorbs at both the 3-fold hollow and the on-top site giving rise to the $T_\perp(NH_3)$ modes at 17.3 and 40.7 meV, respectively. In the large Ru(11$\bar{2}$0) unit cell there is certainly space for two molecules. Applying density functional theory to Ru clusters, Neyman et

al.[23] have calculated the bonding and vibrations of isolated NH_3 molecules on a Ru(0001) plane giving rise to a vibrational energy of 19 meV for the $T_{\perp}(NH_3)$ mode at the 3-fold hollow and of 47 meV for the respective mode at the on-top site. The calculated values are in good agreement with our experimental results for Ru(11$\bar{2}$0) and those for Ru(0001).[22]

Our interpretation is further supported by the observation of two NH_3 α states of different bonding strength in TDS. Whereas on Ru(0001) mostly one α state has been observed, Benndorf and Madey[6] have also distinguished between two α states but suggested that both should be bonded to the 3-fold hollow site with the α_2-NH_3 being tilted to some extent toward the surface. As shown in Figure 5 the TDS observations are well confirmed by the HREELS results: warming to 250 K lets the $T_{\perp 2}(NH_3)$ peak disappear, corresponding to the desorption of the α_2 state, whereas the intensity of the $T_{\perp 1}(NH_3)$ mode remains unchanged. Thus, the α_1 and α_2 states are associated with the desorption of NH_3 adsorbed in 3-fold hollow as well as on-top sites, respectively. The specific arguments proving the adsorption of NH_3 at two different sites in the monolayer are given here for the first time.

The finding, that the on-top site is more weakly bonding than the 3-fold hollow site, is in contradiction to the aforementioned DFT calculations but in line with earlier molecular orbital (MO) calculations.[24] It is contra-intuitive that the stronger bonded α_1 state exhibits the smaller vibration energy (17.3 vs 40.7 meV). This observation can be reconciled by considering that the 3-fold hollow site may exhibit a potential well wider in space leading to a weaker curvature at the bottom and therefore to a smaller transition energy to the first excited vibrational state.

A complete route of the thermal evolution of ammonia with heating to higher temperatures can be given as follows:

$$\alpha_2\text{-}NH_{3,ad} \xrightarrow{170-250\ K} NH_3\uparrow + H_{2,coadsorbed}\uparrow \quad (1)$$

$$\alpha_1\text{-}NH_{3,ad} \xrightarrow{250-300\ K} NH_3\uparrow \quad (2)$$

$$\alpha_1\text{-}NH_{3,ad} \xrightarrow{270-300\ K} NH_{2,ad} + {}^1/_2\, H_{2,\gamma}\uparrow \quad (3)$$

$$NH_{2,ad} \xrightarrow{300-340\ K} NH_{ad} + {}^1/_2\, H_{2,\beta}\uparrow \quad (4)$$

$$NH_{ad} \xrightarrow{340-400\ K} N_{ad} + {}^1/_2\, H_{2,\alpha}\uparrow \quad (5)$$

$$N_{ad} + N_{ad} \xrightarrow{>600\ K} N_2\uparrow \quad (6)$$

These reactions describe that the α_2-NH_3 species desorbs molecularly, whereas the α_1-NH_3 species undergoes desorption or decomposition. The latter channel opens at 270 K and proceeds successively giving rise to NH_2, NH, or N, accompanied by three different H_2 TDS peaks.[17] Atomic nitrogen desorbs associatively for $T > 600$ K.

Here we briefly comment on the hydrogen evolution. We have detected hydrogen from three different sources: (1) Chemisorbed hydrogen as shown in Figure 8, (2) hydrogen from NH_x decomposition according to eqs 3−5,[17] and (3) hydrogen coadsorbed with NH_3 according to eq 1.[17] As shown in Figure 8, chemisorbed hydrogen is characterized by a rather broad second-order desorption peak tailing-off at about 400 K. An appreciable part is from the residual gas and enables overnight NH_3 formation at a N-covered surface. Hydrogen from NH_x decomposition evolves at 275 K ($H_{2,\gamma}$), 325 K ($H_{2,\beta}$), and 375 K ($H_{2,\alpha}$).[17] The peaks of $H_{2,\beta}$ and $H_{2,\alpha}$ are of first order and very sharp indicating that they result from the decomposition and not from coadsorbed H. Finally, about the same amount as in each of the $H_{2,\alpha}$, $H_{2,\beta}$, and $H_{2,\gamma}$ states is coadsorbed with NH_3 and is released at 220 K before any NH_3 decomposition.[17] First of all, this indicates that a saturation amount of NH_3 and its decomposition products blocks H adsorption at temperatures above 220 K; whereas at the bare surface H is adsorbed from the background, at the NH_3-saturated surface H plays a considerable role only below 220 K. This observation also indicates that coadsorbed H is released prior to NH_3 desorption so that the bonding competition effect is not influenced by H coadsorption.

TABLE 3: Activation Energies [kJ/mol] for N_2 Desorption on Different Ru Surfaces

Ru surfaces	Ru(0001) ref 11	Ru(0001) ref 7	Ru(0001) step sites ref 29	Ru(10$\bar{1}$0) ref 28	Ru(11$\bar{2}$1) ref 16	Ru(11$\bar{2}$0) this work
activation energies	190	184	145	120	115	120

We discuss now the reactive site on Ru(11$\bar{2}$0) at which NH_3 dehydrogenation takes place. As mentioned above, this process occurs only for the α_1-NH_3 state, i.e., only at the 3-fold hollow site. From the vibration mode analysis we have concluded[18] that the reaction intermediate NH_2 is titled relative to the surface with a C_s symmetry. Thus, this species is presumably adsorbed also in 3-fold hollow sites accounting for the tilted geometry. Furthermore, we have found that both NH and N are bonded to the two different 3-fold hollow sites (see Figure 1) giving rise to two dipole active δ(NH) and ν(N−Ru) modes, respectively.[18] From the above analysis we suggest that the dehydrogenation reactions of NH_3 on Ru(11$\bar{2}$0) proceed successively at the 3-fold hollow sites which are the reactive ones.

Although the Ru(11$\bar{2}$0) surface turns out to be reactive in NH_3 dehydrogenation, only a rather low N coverage of only 0.11 ML (2.2×10^{14} molecules·cm^{-2}) is achieved following NH_3 exposure at 85 K and annealing.[17] Interestingly, the maximum amount of CO dissociation on Ru(11$\bar{2}$0) is also only about 0.1 ML,[25] equivalent to about one adsorbed molecule per five unit cells. This means that the dissociation occurs only when the four nearest neighboring unit cells are not occupied. This phenomenon can be explained in terms of the bonding competition effect:[26,27] A neighboring species can destabilize the primary molecule and increase its dissociation barrier. When an additional NH_3 molecule is adsorbed in a neighboring unit cell on Ru(11$\bar{2}$0), some surface Ru atoms will take part in the bonding with both NH_3 molecules. Thus, the adsorption bond of the primary NH_3 molecule will be weakened because it has to share the surface charges involved in the adsorption bonds with the neighboring NH_3 molecule. NH_3 usually behaves as an electron donor on metal surfaces and transfers charge from the N lone pair to the metal whose capacity to accept charge—on the other hand—is limited. In the case of coadsorption of NH_3 in the neighboring unit cells, the additional donation from the neighboring NH_3 reduces the charge donation from the first NH_3 thus increasing the dissociation barrier.

Compared to Ru(0001)[10] the thermal stabilization of N is weaker on Ru(11$\bar{2}$0). By applying the Redhead model for second-order desorption kinetics, the activation energy for N_2 desorption was calculated to be 120 ± 20 kJ/mol which is similar to the values derived for Ru(10$\bar{1}$0)[28] and Ru(11$\bar{2}$1)[16] (see Table 3). The efficiency of a catalyst in NH_3 synthesis is determined by several factors among them the velocity of N_2 dissociation and the blocking of the surface by N atoms. The latter factor is weakened for the high-index surfaces compared to Ru(0001). Most importantly, Table 3 shows that the step sites

at Ru(0001) are much more effective than the terrace sites. N_2 desorption from the clean Ru(0001) surface is totally dominated by desorption from steps,[29] and the obtained desorption barrier of 145 kJ/mol is comparable with the values for the high-index surfaces. In an earlier study from our laboratory we arrived at the conclusion that the high-index surfaces are not more effective in N_2 dissociation than the low-index surfaces[12] in agreement with the implication from Table 3.

Finally, NH_3 synthesis from stepwise hydrogenation of adsorbed N atoms is observed here through HREELS. The reaction intermediates NH and NH_2 are clearly identified. A recent DFT calculation[30] revealed that the stepwise addition reactions are important in ammonia synthesis, which means that in order to improve NH_3 synthesis the stepwise hydrogenation reactions cannot be neglected. Certainly, the interaction of hydrogen and nitrogen should be studied in more detail which is, however, beyond our present investigation.

5. Conclusion

NH_3 exposure at 85 K leads to molecular adsorption on the Ru(11$\bar{2}$0)surface. All anticipated vibrational modes for the NH_3 monolayer are identified. Consistent experimental observations of two states of different bonding strength are reported for the first time. The two states are characterized by two translational modes perpendicular to the surface: $T_{\perp 1} = 17.3$ meV for the α_1 state, assigned to a 3-fold hollow site, and $T_{\perp 2} = 40.7$ meV for the more weakly bonded α_2 state assigned to an on-top site. The NH_3 molecule is adsorbed on the Ru(11$\bar{2}$0) surface with a tilted geometry.

Upon annealing to higher temperature, α_2-NH_3 desorbs completely before the channel for NH_3 dehydrogenation is opened at about 270 K. The latter takes place only for α_1-NH_3, in three successive steps at the same site. The Ru(11$\bar{2}$0) surface turns out to be very reactive for NH_3 dehydrogenation. The low nitrogen coverage of 0.11 ML (2.2×10^{14} molecules·cm^{-2}) is attributed to the bonding competition effect which increases the dissociation barrier when a second NH_3 molecule adsorbs in a neighboring unit cell. The activation energy for the associative desorption of nitrogen is estimated to be 120 ± 20 kJ/mol.

NH_3 synthesis from successive hydrogenation of adsorbed N atoms is observed at 300 K as confirmed by the identification of the reaction intermediates NH and NH_2.

Acknowledgment. We thank Professor G. Ertl for support, P. Geng for technical assistance, and M. Richard for editing the manuscript and figures.

References and Notes

(1) Ertl, G. In *Catalytic Ammonia Synthesis*; Jennings, J. R., Ed.; Plenum: New York, 1991; p 109.
(2) K. Aika *Angew. Chem., Int. Ed. Engl.* **1986**, *25*, 558.
(3) Tennison, S. R. In *Catalytic Ammonia Synthesis*; Jennings, J. R., Ed.; Plenum: New York, 1991; p 303.
(4) Danielson, L.; Dresser, M.; Donaldson, E.; Dickinson, J. *Surf. Sci.* **1978**, *71*, 599.
(5) Danielson, L.; Dresser, M.; Donaldson, E.; Sandstrom, D. *Surf. Sci.* **1978**, *71*, 615.
(6) Benndorf, C.; Madey, T. *Surf. Sci.* **1983**, *135*, 164.
(7) Tsai, W.; Weinberg, W. H. *J. Phys. Chem.* **1987**, *91*, 5302.
(8) Egawa, C.; Naito, S.; Tamaru, K. *Surf. Sci.* **1984**, *138*, 279.
(9) Parmeter, J. E.; Wang, Y.; Mullins, C. B.; Weinberg, W. H. *J. Chem. Phys.* **1988**, *88*, 5225.
(10) Shi, H.; Jacobi, K.; Ertl, G. *J. Chem. Phys.* **1993**, *99*, 9248.
(11) Shi, H.; Jacobi, K.; Ertl, G. *J. Chem. Phys.* **1995**, *102*, 1432.
(12) Dietrich, H.; Geng, P.; Jacobi, K.; Ertl, G. *J. Chem. Phys.* **1996**, *104*, 375.
(13) Dahl, S.; Logadottir, A.; Egeberg, R. C.; Larsen, J. H.; Chorkendorff, I.; Törnqvist, E.; Norskov, J. K. *Phys. Rev. Lett.* **1999**, *83*, 1814.
(14) Jacobi, K. *Phys. Status Solidi A* **2000**, *177*, 37.
(15) Wang, J.; Wang, Y.; Jacobi, K. *Surf. Sci.* **2001**, *482*−*485*, 153.
(16) Jacobi, K.; Wang, Y.; Fan, C. Y.; Dietrich, H. *J. Chem. Phys.* **2001**, *115*, 4306.
(17) Wang, Y.; Lafosse, A.; Jacobi, K. *Surf. Sci.* **2002**, *507*−*510*, 773.
(18) Wang, Y.; Jacobi, K. *Surf. Sci.* **2002**, *513*, 83.
(19) Nakamoto, K. *Infrared and Raman Spectra of Inorganic and Coordination Compounds, Part B*; Wiley: New York, 1997.
(20) Ibach, H.; Mills, D. L. *Electron Energy Loss Spectroscopy and Surface Vibrations*; Academic: New York, 1982; p 348.
(21) Toennies, J. P.; Wöll, Ch.; Zhang, G. *J. Chem. Phys.* **1992**, *96*, 4023.
(22) Widdra, W.; Moritz, T.; Kostov, K. L.; König, P.; Staufer, M.; Birkenheuer, U. *Surf. Sci.* **1999**, *430*, L558.
(23) Neyman, K. M.; Staufer, M.; Nasluzov, V. A.; Rösch, N. *J. Mol. Catal. A* **1997**, *119*, 245.
(24) Rodriguez, J. A.; Truong, C. M.; Goodman, D. W. *J. Vac. Sci. Technol., A* **1992**, *10*, 955.
(25) Wang, J.; Wang, Y.; Jacobi, K. *Surf. Sci.* **2001**, *488*, 83.
(26) Liu, Z. P.; Hu, P.; Alavi, A. *J. Chem. Phys.* **2001**, *114*, 8244.
(27) Fan, C. Y.; Bonzel, H. P.; Jacobi, K. *J. Chem. Phys.* **2003**, *118*, 9773.
(28) Dietrich, H.; Jacobi, K.; Ertl, G. *J. Chem. Phys.* **1997**, *106*, 9313.
(29) Dahl, S.; Törnqvist, E.; Chorkendorff, I. *J. Catal.* **2000**, *192*, 381.
(30) Zhang, C.; Liu, Z. P.; Hu, P. *J. Chem. Phys.* **2001**, *115*, 609.